

Interpretation of galaxy rotation curves from primordial black holes in 4D Einstein-Gauss-Bonnet gravity

M. Bousder*

LPHE-MS Laboratory, Department of physics,
Faculty of Science, Mohammed V University in Rabat, Morocco

August 9, 2022

Abstract

We develop a novel approach to the dark matter halos in the context of 4 dimensional Einstein–scalar-Gauss-Bonnet gravity to reproduce the flat rotation curves of galaxies. Moreover, the Gauss-Bonnet coupling describes the interior structure of the galaxies, while there is a presence of a scalar field ϕ in the galaxy edges. This can provide an interesting interpretation for the functional coupling $f(\phi)$. We discuss how this comparison can naturally drive the observed percentages of matter and dark matter in the Universe. The effective mass range in our model is $10^{-2}kg - 10^3kg$, which is in good agreement with the constraints on primordial black holes.

Keywords: Galaxy, rotation curves, primordial black holes, Einstein-Gauss-Bonnet gravity

1 Introduction

The first accepted evidence for the existence of dark matter in the galaxy rotation curves [1, 2, 3]. It is well known that the orbital velocities V of planets in planetary systems decline with distance according to Kepler’s third law [4] $V^2 = GM/r$. While the rotational velocity of the galaxy almost stays consistently among all galaxies [5, 6]. The rotational speeds of stars inside the galaxy do not follow the rules found in smaller orbital systems.

*mostafa.bousder@um5.ac.ma

The effective potential can be used to determine the orbits of planets [7], also in the cosmological evolution analysis of the scalar field, allowing the detection of dark energy in orbit [8]. In Modified Newtonian Dynamics (MOND), the rotation curves of spiral galaxies are asymptotically flat [9] and imply a mass-velocity relationship as $V^D \propto M$, with D is in the neighborhood of 4 [13]. It is known that some interesting phenomena of galaxies, like the relationship between the rotation velocity in spiral galaxies and the luminosity [14]. According to the MOND theory, the rotational velocity of stars around a galaxy at large distances is $V_{\max}^4 \sim GMa_0$, where $a_0 \approx 1, 2 \times 10^{-10} \text{ms}^{-2}$ is a fundamental acceleration scale of nature, and M is the total mass of a galaxy. It is treated as a point mass at its center, providing a crude approximation for a star in the outer regions of a galaxy. The V_{\max}^4 predicts that the rotational velocity is constant out to an infinite range and that the rotational velocity doesn't depend on a distance scale but the magnitude of the acceleration a_0 . Additionally, the amplitude and scale of the initial fluctuations describe the formation of galactic halos in a flat universe dominated by cold dark matter (CDM) [10]. Massive halos form preferentially in regions of high dark matter density. The formation of dark halos is under the assumption that the CDM particles have a finite cross section for elastic collisions [11]. Their formation sites correspond well to high peaks of the initial linear density field. In the galactic nuclei, a possible explanation for the formation of the supermassive black holes at the galaxy center is caused by the collapse of a large number of stars' high concentrations at the galaxy center. To describe the formation of protogalaxies, it's useful to use the second-order phase transition in the inflation stage [12].

Recently, the 4D Einstein-Gauss-Bonnet (EGB) theory [21] provides a new insights into the 4-dimensional (4D) theory of gravity. It is in contradiction with the Lovelock theorem [22] which describes the gravity at $D \geq 5$. The idea of the 4D EGB gravity is rescaling first the Gauss-Bonnet coupling constant by the factor $1/(D-4)$, then taking the limit $D \rightarrow 4$. The divergent factor $1/(D-4)$ is canceled by the vanishing GB contributions, which leads to a theory of gravity with only two dynamical degrees of freedom. However, the idea of the limit $D \rightarrow 4$ is not clearly defined [23, 24, 25, 26]. It was explicitly confirmed by a direct product D -dimensional spacetime or by adding a counter term, before taking the limit $D \rightarrow 4$, which can be seen as a class of Horndeski theory [27]. Although the EGB gravity is currently debatable, the spherically symmetric black hole solution is still meaningful and worthy of study [28]. In [16] we have studied the relationship between the MOND paradigm and scalar-Gauss-Bonnet (EsGB) gravity, we added a new relativistic part to the MOND from EsGB gravity.

Motivated by these, the purpose of the present paper is to introduce a difference between the physical quantities in the interior (ex: interior of galaxies) and the edge (ex: dark

matter halos). We will also point out that there is the presence of two gravitational constants, the first is that of Newton's constant, the second appears more for very intense gravity (like galaxies). We will show why the values of the constant θ_0 in [16] for the dwarf spheroidal and irregular dwarf galaxies are not constant. We show the presence of primordial black holes in the dark matter halos according to the rotation curves of galaxies.

In section 2, we briefly review the Einstein-Gauss-Bonnet gravity in 4-dimensions in coupling with a scalar field. In Section 3, we study the effective mass of this scalar field and its relation to the rotation curves of galaxies. In Section 4, we study the galaxy formation from primordial black holes. In Section 5, we summarize our conclusions.

2 Dark halos in Einstein-Gauss-Bonnet gravity

The EGB gravity is a higher derivative terms of the Lovelock gravity. In this section, we explain in detail how to construct the equation of motion of the Einstein-scalar-Gauss-Bonnet (EsGB) gravity. We begin by reviewing the 4D EsGB action [29]

$$\mathcal{S} = \frac{1}{2\kappa^2} \int \sqrt{-g} d^4x \left(\mathcal{L} - \frac{1}{2} g^{\mu\nu} \partial_\mu \phi \partial_\nu \phi - \mathcal{V}(\phi) \right) + \mathcal{S}_m. \quad (2.1)$$

The EsGB lagrangian is given $\mathcal{L} = R + f(\phi)(R^2 - 4R_{\mu\nu}R^{\mu\nu} + R_{\mu\nu\rho\sigma}R^{\mu\nu\rho\sigma})$, where $1/\kappa^2 = 1/8\pi G_N = 1.221 \times 10^{19} GeV$ is the reduced Planck mass, R is the Ricci scalar, \mathcal{S}_m is the matter action and $f(\phi)$ is a functional coupling of the scalar field ϕ . In the above equation $(\mu, \nu) = (0, 1, 2, 3)$. The variation with respect to the field ϕ gives us the equation of motion for the scalar field

$$\square \phi = \partial_\phi \mathcal{V}_{eff}(\phi), \quad (2.2)$$

where $\square \equiv \nabla_\mu \nabla^\mu$ and the effective potential is

$$\mathcal{V}_{eff}(\phi) = \mathcal{V}(\phi) - f(\phi) \mathcal{G}. \quad (2.3)$$

Varying the action (2.1) over the metric $g_{\mu\nu}$, we obtain the following equations of motion:

$$G^{\mu\nu} + \mathcal{K}^{\mu\nu} + f(\phi) \mathcal{H}^{\mu\nu} + \frac{1}{2} [\mathcal{T}_\phi^{\mu\nu} - g^{\mu\nu} \mathcal{V}_{eff}(\phi)] = \frac{1}{2} \kappa^2 T^{\mu\nu}, \quad (2.4)$$

where the Einstein tensor is $G^{\mu\nu} = R^{\mu\nu} - \frac{1}{2} g^{\mu\nu} R$, the matter stress tensor is $T^{\mu\nu} = -\frac{2}{\sqrt{-g}} \frac{\delta \mathcal{S}_m}{\delta g_{\mu\nu}}$. On the other hand, the $\mathcal{K}^{\mu\nu}$ and $\mathcal{H}^{\mu\nu}$ are given by

$$\mathcal{K}^{\mu\nu} = 4 \left[G^{\mu\nu} \square + \frac{1}{2} R \nabla^\mu \nabla^\nu + (g^{\mu\nu} R^{\rho\sigma} - R^{\mu\rho\nu\sigma}) \nabla_\rho \nabla_\sigma - R^{\nu\rho} \nabla_\rho \nabla^\mu + R^{\mu\rho} \nabla_\rho \nabla^\nu \right] f(\phi), \quad (2.5)$$

$$\mathcal{H}^{\mu\nu} = 2R^{\mu\rho\sigma\tau}R^\nu_{\rho\sigma\tau} - RR^{\mu\nu} + \frac{1}{2}R^\mu_\rho R^{\nu\rho} - R^{\mu\rho\sigma\tau}R^\nu_{\rho\sigma\tau}. \quad (2.6)$$

The tensor $\mathcal{K}^{\mu\nu}$ represents an operator which acts on $f(\phi)$. The energy-momentum tensor for the scalar field is

$$\mathcal{T}_\phi^{\mu\nu} = \nabla^\mu\phi\nabla^\nu\phi - \frac{1}{2}g^{\mu\nu}\nabla_\rho\phi\nabla^\rho\phi. \quad (2.7)$$

The form the functional $f(\phi)$ can take $f(\phi) \propto e^{-\gamma\phi}$ [30], where γ is a constant, which corresponds to EGB gravity coupled with dilaton that arises as a low-energy limit of the string theory [31]. The motion of compound objects in an external field of the galaxy like the globular clusters is independent of its internal structure and may be described in the MOND limit [32]. We assume that in the galaxies edges (dark halos), there is a presence of a scalar field ϕ , while inside the galaxy is replaced by the Gauss-Bonnet (GB) coupling α as

$$\begin{aligned} \text{coupling constant} &= f(\phi), & \text{galaxy edges } (D = 4) \\ \text{coupling constant} &= \frac{\alpha}{D-4}, & \text{galaxy interior } (D \rightarrow 4) \end{aligned} \quad (2.8)$$

The GB coupling α is measured in km^2 . In the galaxies interior, we have rescaled the coupling constant $\alpha \rightarrow \alpha/(D-4)$. The negative (positive) α leads to a decrease (increase) of the galaxy radius and the maximum mass [33]. If $\alpha < 0$ the solution is still the anti-de Sitter (AdS) space, if $\alpha > 0$ the solution is the de Sitter (dS) space [34].

We investigate in detail the impact of the Gauss-Bonnet coupling on properties of the galaxies, such as mass, radius and density. Considering the limit $D \rightarrow 4$, it has an effect on gravitational dynamics in 4D. Additionally, at the galaxy boundary ($r = r_{\max}$), the GB coupling must be continuous, i.e. $f(\phi) \rightarrow \frac{\alpha}{D-4}$. On the other hand, the function $f(\phi)$ describes the star exterior region. To study the equations of motion inside and outside the galaxy, we differentiate between two cases:

In galaxy interior ($D \rightarrow 4$) we have:

$$G^{\mu\nu} + \alpha \left(\mathcal{H}^{\mu\nu} + \frac{1}{2}g^{\mu\nu}\mathcal{G} \right) = \frac{\kappa^2}{2}T^{\mu\nu}. \quad (2.9)$$

In galaxy edges ($D = 4$) we have:

$$G^{\mu\nu} + \mathcal{K}^{\mu\nu} + f(\phi) \left[\mathcal{H}^{\mu\nu} - \frac{1}{2f(\phi)}g^{\mu\nu}(\nabla_\lambda\phi\nabla^\lambda\phi + 4\mathcal{V}_{eff}(\phi)) \right] = \frac{1}{2}\kappa^2T^{\mu\nu}, \quad (2.10)$$

with $g_{\mu\nu}\mathcal{T}_\phi^{\mu\nu} = -\nabla_\lambda\phi\nabla^\lambda\phi$. In galaxy interior ($D \rightarrow 4$) we have: the GB invariant can be greatly simplified to the matter density [35, 15]. By comparing, Eq.(2.9) and Eq.(2.10), we notice that the term $(\nabla_\lambda\phi\nabla^\lambda\phi + 4\mathcal{V}_{eff}(\phi))/f(\phi)$ represents a density. Using Eq.(2.3) we obtain

$$\begin{aligned} \rho_{DM} &\equiv 4\mathcal{G} - \frac{4}{f(\phi)} \left(\frac{1}{4}\nabla_\lambda\phi\nabla^\lambda\phi + \mathcal{V}(\phi) \right), & \text{galaxy edges } (D = 4) \\ \rho_m &= \mathcal{G}, & \text{galaxy interior } (D \rightarrow 4) \end{aligned} \quad (2.11)$$

where $\rho_m(r)$ is the density of matter enclosed within r , and ρ_{DM} is the density of dark matter halo surrounding the galaxy. Note that the relation between ρ_{DM} and ρ_m highlight the chameleon dark matter [36, 37]. For $\mathcal{V}(\phi) \approx -\frac{1}{4}\nabla_\lambda\phi\nabla^\lambda\phi$, we obtain $\rho_{DM} \approx 4\rho_m$, which is in good agreement with the observation data of the percentages of dark matter and the matter in the Universe [38]: $\rho_{DM} \equiv 80\%$ and $\rho_m \equiv 20\%$. In this profile, the density $4\rho_m - \rho_{DM}$ represents the small variation of the DM density according to the dynamics of the field ϕ .

3 Rotation curves of galaxies

The scalar field sits at the minimum of its effective potential. We assume that a massive scalar field begins oscillating about a minimum. The mass of small fluctuations around ϕ_{\min} gives a new scalar field mass as effective mass by

$$M_{eff}^2 = \left. \frac{\partial^2}{\partial\phi^2}\mathcal{V}_{eff}(\phi) \right|_{\phi=\phi_{\min}}. \quad (3.1)$$

The effective mass is expressed in the following way

$$M_{eff} = \sqrt{\frac{\partial^2\mathcal{V}(\phi_{\min})}{\partial\phi^2} - \rho_m \frac{\partial^2 f(\phi_{\min})}{\partial\phi^2}}. \quad (3.2)$$

This equation is in good agreement with the expression for the effective mass in [19, 20]. At the end of inflation scenario [19], the mass M_{eff} is described by sinusoidal functions by the quantum fluctuations. During each oscillation of the field ϕ , the effective mass M_{eff} is much greater than the inflaton mass $\sqrt{\rho_m \partial^2 f(\phi_{\min})/\partial\phi^2}$. Therefore, the resonance of ϕ begins at the end of inflation with the typical frequency of oscillation $\omega(t) \sim \sqrt{M_{eff}^2(t) + \rho_m \partial^2 f(\phi_{\min})/\partial\phi^2}$. For very small ϕ there is a change in the frequency of oscillations $\omega(t)$ and the system becomes adiabatic. From Eq. (3.2), we notice the existence of the condition:

$$\rho_m \leq \frac{\mathcal{V}''(\phi_{\min})}{f''(\phi_{\min})}, \quad (3.3)$$

with (\prime) represent $\partial/\partial\phi$. Taking $\rho_{\max} = \mathcal{V}''(\phi_{\min})/f''(\phi_{\min})$, with ρ_{\max} represents the maximum mass of ordinary matter in the galaxy. Using Eqs. (3.2,3.3) we find

$$M_{eff} = \sqrt{\frac{\partial^2 f(\phi_{\min})}{\partial\phi^2}} \sqrt{\rho_{\max} - \rho_m(r)}, \quad (3.4)$$

where $\rho_m(r)$ is the local matter energy density and $f(\phi_{\min})$. We notice that $\rho_{\max} - \rho_m(r) \sim M_{eff}^2 \sim (\text{rotation velocity})^4$. For the elliptical galaxy, we use the power-law relation between the luminosity L and the central stellar velocity dispersion σ of Faber-Jackson relation: $L \propto \sigma^D$, where D is in the neighborhood of 4 and σ is the stellar

velocity dispersion. While for the spiral galaxy we use the Tully–Fisher relation (TFR), it is a relationship between the mass (intrinsic luminosity) and its asymptotic rotation velocity. The gravitational potential is writing as $\nabla^2 V = 4\pi G\rho_m$ [39]. Using the mass-velocity relationship as is shown in [16], we notice that $\sqrt{\partial^2 f(\phi_{\min})/\partial\phi^2} = GM/KV^2$, where V is the rotation velocity of the galaxy disk and K is a constant, which roughly equals $K \approx 69.44kg^{-1/2}km^{-1/2}$ and $\theta_0 = (KM_{eff})^{-1/2}$ [16]. The total mass of the galaxy M is integrated mass within some the galaxy radius r_{\max} as $M = \int_0^{r_{\max}} 4\pi r^2 \rho_m(r) dr$. Notice that we have $\rho_m(r_{\max}) \neq \rho_{\max}$. It is clear from the expression in Eq. (3.4) that

$$M_{eff}V^2 = \frac{GM}{K} \sqrt{\rho_{\max} - \rho_m(r)}. \quad (3.5)$$

This expression of M_{eff} is in good agreement with the masses of the produced PBHs following the critical scaling in [17, 18]. The effective mass M_{eff} may represent the mass of the primordial black hole. To verify this, we calculate the masses M_{eff} for some galaxies; see tables (1) and (1). We found that this mass varied in the interval $M_{eff} \sim 10^{-2}kg - 10^3kg$, which is in good agreement with the constraints on the fraction of the Universe that may have gone into PBHs over the mass range $10^{-8}kg - 10^{47}kg$ [51]. We note that the term $M_{eff}V^2/2$ is the kinetic energy of field ϕ . Additionally, since V is the galaxy rotation velocity, then this field is responsible for the galaxies rotation. In the limit of $KM_{eff} = r\sqrt{\rho_{\max} - \rho_m(r)}$ we can only recover the corresponding Poisson equation for Newtonian velocity $V^2 = GM/r$. In the galaxy edges, the local density of ordinary matter $\rho_m(r)$ is very low, from which, we obtain

$$V_{\max} = \left(\frac{GM}{KM_{eff}} \right)^{1/2} \rho_{\max}^{1/4}, \quad (3.6)$$

where V_{\max} is the maximum rotation velocity of the galaxy. According to this relation, the Milgrom constant a_0 is no longer constant, but it depends on other parameters like the mass of the galaxy and the effective mass. If M_{eff} is nearly constant, the V_{\max} is completely flat. There are two gravitational constants (G, K). This means that in the limit of low mass (sun, stars, planets), the KM_{eff} term will be very weak. For the galaxy and galaxy clusters masses, the term KM_{eff} will be more important and will have an impact on the rotation curves. It is possible that DM does not consist of a particle, but we just must to find a theory of gravity beyond general relativity [15].

LS galaxies	$\rho(\times 10^{-22}kg/m^2)$	$M_{in}(\times 10^{10}M_{\odot})$	$V_{max}(km/s)$	$\theta_0(kg^{-1/4}km^{1/4})$	$M_{eff}(kg)$
Milky Way	13, 10	12, 10	220	0, 086	1.94
NGC 7331	8, 70	14, 70	268.1	0, 105	1.30
NGC 4826	45, 00	1, 90	180.2	0, 130	0.85
NGC 6503	18, 40	0, 958	121	0, 154	0.61
NGC 7793	12, 00	0, 88	117.9	0, 174	0.47
UGC 2885	15, 30	11, 70	300	0, 114	1.11
NGC 253	10, 00	4, 30	229	0, 160	0.56
NGC 925	8, 60	2, 00	113	0, 120	1
NGC 2403	5, 20	2, 90	143.9	0, 144	0.69
NGC 2841	8, 02	17	326	0, 121	0.98
NGC 2903	6, 30	6, 70	215.5	0, 135	0.79
NGC 3198	3, 26	6, 00	160	0, 125	0.921
NGC 5585	10, 1	0, 59	92	0, 173	0.48
NGC 4321	8, 80	16, 8	270	0, 098	1.49
MS galaxies	$\rho(\times 10^{-22}kg/m^2)$	$M_{in}(\times 10^{10}M_{\odot})$	$V_{max}(km/s)$	$\theta_0(kg^{-1/4}km^{1/4})$	$M_{eff}(kg)$
NGC 4303	6, 81	3, 68	150	0, 124	0.93
NGC 5055	5, 21	7, 07	215	0, 138	0.75
NGC 4736	14, 00	1, 77	198.3	0, 198	0.36
NGC 5194	1, 00	4, 00	232	0, 299	0.16
NGC 4548	3, 20	3, 80	290	0, 287	0.17
L and E Galaxies	$\rho(\times 10^{-22}kg/m^2)$	$M_{in}(\times 10^{10}M_{\odot})$	$V_{max}(km/s)$	$\theta_0(kg^{-1/4}km^{1/4})$	$M_{eff}(kg)$
UGC 3993	3, 10	17.8	300	0, 138	0.75
NGC 7286	4, 60	0.59	98	0, 224	0.28
NGC 2768	10, 00	1.98	260	0, 268	0.20
NGC 3379	0, 90	1.10	60	0, 151	0.63
NGC 2434	1, 00	5.00	231	0, 266	0.20
NGC 4431	13, 00	0.30	78	0, 193	0.38

Table 1: Large spirals (LS) galaxies, Messier Spirals (MS), Lenticular and Elliptical (L and E) Galaxies.

Id galaxies	$\rho(\times 10^{-22}kg/m^2)$	$M_{in}(\times 10^{10}M_{\odot})$	$V_{max}(km/s)$	$\theta_0(kg^{-1/4}km^{1/4})$	$M_{eff}(kg)$
WLM (DDO 221)	0,92	0,00863	19	0,539	0.049
M81dWb	5,00	0,007	28,5	0,588	0.041
Holmberg II	3,64	0,0428	34	0,307	0.152
NGC 3109	8,00	0,0299	67	0,605	0.039
NGC 4789a	93,00	0,0188	50	0,303	0.156
NGC 3034	22,00	1,00	137	0,163	0.542

dSphs Galaxies	$\rho(\times 10^{-22}kg/m^2)$	$M_{in}(M_{\odot})$	$V_{max}(km/s)$	$\theta_0(kg^{-1/4}km^{1/4})$	$M_{eff}(kg)$
Carina	6,50	3.38×10^6	8,5	0,007	293.89
Leo I	13,60	7.74×10^6	12,5	0,006	400.02
Draco	7,40	3.40×10^6	12	0,01	144.00
Fornax	0,373	12.40×10^6	11,5	0,01	144.00

Table 2: Irregular dwarf (Id) galaxies and dwarf spheroidal (dSphs) galaxies

By comparing the two tables 1 and 2, we notice that the mass M_{eff} is almost constant and small for the spirals galaxies, while, it is very important for the dwarf spheroidal galaxies (dSphs) [49]. This shows why the rotation curves of the spirals galaxies are almost static. However, the curves of dSphs increase relatively to the galactic center [48], which justifies the major presence of the dark matter in dSphs [50]. So, there is an interesting connection between the parameters M_{eff} and the amount of dark matter in each galaxy. This adds a new physical parameter to Eq. (3.6), i.e. the mass M_{eff} is among the physical parameters of the galaxy in this model. M_{eff} varied from one type of galaxy to another, which shows that M_{eff} is a parameter that can determine the type of a galaxy if we know his rotational velocity. Also, permit us to determine the rotational velocity if we know the type of galaxy. From the observation data of galaxies, we trace the evolution of θ_0 and M_{eff} according to the types of galaxies Fig. (1) and Fig. (2).

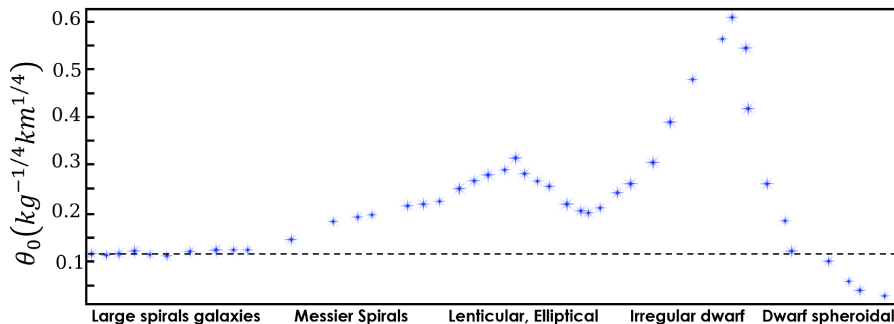


Figure 1: Evolution of $\theta_0 = (KM_{eff})^{-1/2}$ as a function of type of galaxies.

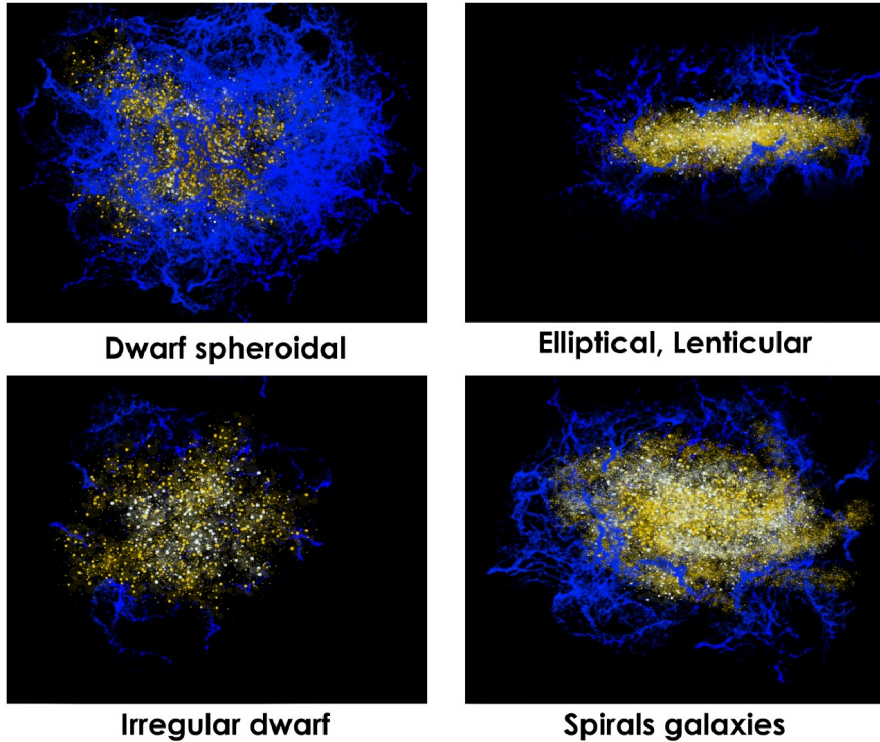


Figure 2: A representation of the evolution of M_{eff} as a function of type of galaxies. The dark matter halo is described by the value of M_{eff} . The blue color represents the halo of dark matter and the white color represents the matter of the galaxies.

According to Fig. (1), the mass parameter M_{eff} describes the evolution and formation of galaxies. The $K M_{eff}$ in Fig. (1) should deviate systematically from $K \approx 69.44 kg^{-1/2} km^{-1/2}$ according to the variation of M_{eff} . This shows that the parameter M_{eff} plays an important role in describing both the rotation and the type of galaxies. The evolution of M_{eff} is done according to categories of galaxies. This shows that dark matter changes from one type to another type of galaxies. We introduce the effective density

$$\rho_{eff}(r) = \rho_{\max} - \rho_m(r) = \left(\frac{K M_{eff}}{r} \right)^4. \quad (3.7)$$

The effective density $\rho_{eff} \sim M_{eff}^4$ is of order 4, which corresponds to the Standard Model (SM) radiation energy density: $\rho_R = \frac{\pi^2}{30} g_* T^4$, where g_* denotes the effective number of relativistic degrees of freedom at reheating time. In this case, the density describes the DM-gas interaction with a typical emission temperature. During the radiation dominated era, the evolution of ρ_{eff} can thus lead to PBH production the density, see next section. As is shown in [45], the radiation density depends on scale factor as $\rho_R \propto a^{-4}$ in the era of radiation dominance, while the PBH density checked $\rho_{PBH} \propto a^{-3}$. So, M_{eff} depends on the redshift z as $M_{eff} \propto a = 1/(1+z)$. This shows a link between dark matter (M_{eff}) and the redshift of a halo which is in good agreement as is shown in [47].

4 Galaxy formation from primordial black holes

In cosmological and quintessence behavior [40, 41], the energy density ρ_ϕ and pressure P_ϕ of the scalar field are given by

$$\rho_\phi = \frac{1}{2}\dot{\phi}^2 + \mathcal{V}(\phi), \quad P_\phi = \frac{1}{2}\dot{\phi}^2 - \mathcal{V}(\phi). \quad (4.1)$$

The quintessence models describe the dark energy with a scalar field ϕ . In this case, ρ_ϕ and P_ϕ are respectively, the density and the pressure of the dark energy (DE). Next, we assume that $\phi = \phi(t)$, i.e. $\nabla_\lambda \phi \nabla^\lambda \phi = \dot{\phi}^2$. Starting from Eqs. (2.11,4.1), we obtain, the density of dark matter profile:

$$\rho_{DM} = 4\rho_m + \frac{1}{f(\phi)} (P_\phi - 3\rho_\phi). \quad (4.2)$$

For small $f(\phi)$, the DM density depends only on $(P_\phi - 3\rho_\phi)/f(\phi)$. To study the stability of the DM under scalar field perturbations, we employ the effective sound speeds $c_\phi^2 = \delta P_\phi / \delta \rho_\phi$. The effective sound speeds are related to the energy density and the pressure, which checked the causality condition $0 \leq c_\phi^2 \leq c^2$. From Eqs. (2.3,4.1,4.2) we obtain

$$M_{eff}^2 = \frac{1}{2} \frac{\partial^2}{\partial \phi^2} \left(\rho_\phi - P_\phi - \frac{\rho_m}{\rho_{DM} - 4\rho_m} (P_\phi - 3\rho_\phi) \right)_{\phi=\phi_{min}}. \quad (4.3)$$

From Eq. (4.2), the functional coupling is given by the dimensionless fraction

$$f(\phi) = \frac{P_\phi - 3\rho_\phi}{\rho_{DM} - 4\rho_m}. \quad (4.4)$$

In the galaxy interior, we assume that $\rho_{DM} \approx 0$ and $P_\phi \approx 0$, so we get $f(\phi) \approx 3\rho_\phi/4\rho_m$. Since ρ_ϕ represents the density of DE according to quintessence, the effect of DE is weak in the galaxy edges, which shows that $f(\phi) (\propto \rho_\phi) \rightarrow 0$. Since the field ϕ exists in the galaxy edges, so, inside the galaxy, we have $(P_\phi = \rho_\phi = 0)$, i.e. $f(\phi) = 0$, which exactly corresponds with the assumption Eq. (2.8). For this reason, we exclude $f(\phi)$ inside galaxies, and we replace it with the GB coupling α . Note the existence of two branches for the dark halo (DH) fraction $f_{DH}(\phi)$ in the galaxy edges ($\rho_m \approx 0$ [46]), depending on the sign chosen as

$$f_{DH}(\phi) = (\omega_\phi - 3) \frac{\Omega_\phi}{\Omega_{DM}}, \quad (4.5)$$

where $\Omega_\phi = \rho_\phi/\rho_{crit}$ and $\Omega_{DM} = \rho_{DM}/\rho_{crit} = 0.26$ [38] is the current DM density parameter. In the context of dark energy (DE), the scalar field requiring $\omega_\phi = P_\phi/\rho_\phi \approx -1$. The Planck Collaboration results [38] provides a constraints on the DE equation of state $\omega_\phi \approx -1.028 \pm 0.032$, i.e. $f_{halos}(\phi) \leq 0$. Since the field ϕ represents the DM halos, then this DE- ω_ϕ proposition is not valid. We recall that the Eq. (3.2) is in good agreement with the expression for the effective mass in [19, 20], which generates a

relationship between the primordial black holes (PBHs) and DM. It is argued that the PBHs could be the origin of the dark matter halos [44, 42]. The PBHs might form a considerable fraction of the DM (contribute more than 10% of the dark matter) [43, 20], the field ϕ may describes the fraction of PBHs. We recall that the PBH fraction defined as $f_{PBH} = \Omega_{PBH}/\Omega_{DM} < 1$, where Ω_{PBH} is the PBH abundance. We assume that $\Omega_\phi = \Omega_{PBH}$, yield

$$f_{PBH} = \frac{f_{DH}(\phi)}{\omega_\phi - 3}. \quad (4.6)$$

The DH function $f_{DH}(\phi)$ describes the PBH fraction if and only if $\omega_\phi > 3$. The formation of galaxies is mainly due to the PBHs. In this scenario, the effective density Eq. (3.7) could be the radiation density due to the PBH evaporation as the Hawking radiation. There is a way to relate the PBHs fraction to the GB coupling, by setting $\omega_\phi = 3D/4$. In the present context, we assume that there is a continuity between $f(\phi)$ and α in galaxy edges, Eq.(2.8). We can express the PBH fraction as follows $f_{PBH} = 4f_{DH}(\phi)/3(D-4)$. By analogy, we observe that $f(\phi) \equiv f_{PBH}$ and $\alpha \equiv \frac{4}{3}f_{DH}(\phi)$. In the galaxy interior ($\rho_{DM} \approx 0$, $P_\phi \approx 0$) so we get $f(\phi) \approx 3\rho_\phi/4\rho_m$. In this case, the relation (4.6) is not valid only in the edges of the galaxy.

5 Conclusion

In summary, we have studied the model describing the rotation curves of galaxies surrounded by scalar dark matter in 4D Einstein-Gauss-Bonnet gravity. We have made a comparison between the galaxy interior and its edges. In this case, the Gauss-Bonnet coupling describes the interior structure of the galaxy, while the coupling function $f(\phi)$ describes the galaxy edges. Under this premise and within the framework of the singlet scalar dark matter (DM) model, we have explored the impact of primordial black holes on the galaxy's formation at early times. The flat galactic rotation curves can be explained either by introducing the Gauss-Bonnet coupling. We show that the difference between the rotation curves of spiral and dwarf galaxies due to the effective mass varied from one type of galaxy to another. So, this mass can determine the type of a galaxy if we know its rotational velocity. The predictions for the galaxy rotation curves from observations and our model agree remarkably for almost all of the 35 galaxies. The effective mass range in our model is $10^{-2}kg - 10^3kg$, which is in good agreement with the constraints on primordial black holes, which shows that the mass hidden in the dark matter halos is a mass of the primordial black holes. This opens a new window on the galaxy's formation in the early Universe by PBHs production.

References

- [1] Rubin, V. C., Ford Jr, W. K., & Thonnard, N., 1980, *Astrophys. J.*, 238, 471-487.
- [2] Rubin, V. C., & Ford Jr, W. K, 1970, *Astrophys. J.*, 159, 379.
- [3] Sofue, Y., & Rubin, V., 2001, *Annu. Rev. Astron. Astrophys.*, 39(1), 137-174.
- [4] Gingerich, Owen. 1975, *Vistas Astron.* 18 : 595-601.
- [5] Rubin, V. C., W. Kent Ford Jr, and Norbert Thonnard. 1980, *Astrophys. J.*, 238 : 471-487.
- [6] Seljak, Uroš. 2000, *Mon. Not. Roy. Astron. Soc.*, 318.1: 203-213.
- [7] Jiang, Yu, and Hexi Baoyin. 2014, *J. Astrophys. Astron.*, 35.1 : 17-38.
- [8] Brax, Philippe, et al. 2004, *Phys. Rev. D*, 70.12 : 123518.
- [9] Milgrom, M., 1983, *Astrophys. J.*, 270, 365-370.
- [10] Frenk, C. S., White, S. D., Davis, M., & Efstathiou, G., 1988, The formation of dark halos in a universe dominated by cold dark matter, *Astrophys. J.*, 327, 507-525.
- [11] Yoshida, N., Springel, V., White, S. D., & Tormen, G., 2000, Weakly self-interacting dark matter and the structure of dark halos. *Astrophys. J.*, 544(2), L87.
- [12] Rubin, S. G., Sakharov, A. S., & Khlopov, M. Y., 2001, *J. Exp. Theor. Phys.*, 92(6), 921-929.
- [13] Sanders, R. H., & McGaugh, S. S., 2002, *Annu. Rev. Astron. Astrophys.*, 40(1), 263-317.
- [14] Aaronson, M., et al., 1982, *The Astrophys. J., Suppl. Ser.*, 50, 241-262.
- [15] Vagnozzi, S. 2017, *Class. Quantum Gravity*, 34(18), 185006.
- [16] Bousder, M. 2022, *Journal of Cosmology and Astroparticle Physics*, 2022(01), 015.
- [17] Vaskonen, V., & Veermäe, H., 2021, *Phys. Rev. Lett.*, 126(5), 051303.
- [18] De Luca, V., Franciolini, G., & Riotto, A., 2021, *Phys. Rev. Lett.*, 126(4), 041303.
- [19] Kofman, L., Linde, A., & Starobinsky, A. A. 1997, *Phys. Rev. D* , 56(6), 3258.
- [20] Wu, Y. P., Pinetti, E., & Silk, J., 2022, *Phys. Rev. Lett.*, 128(3), 031102.

- [21] Glavan, D., & Lin, C., 2020, Phys. Rev. Lett., 124(8), 081301.
- [22] Lovelock, D, 1972, J. Math. Phys. 13(6), 874-876.
- [23] Bonifacio, J., Hinterbichler, K., & Johnson, L. A., 2020, Phys. Rev. D, 102(2), 024029.
- [24] Gürses, M., Şişman, T. Ç., & Tekin, B., 2020, Phys. Rev. Lett., 125(14), 149001.
- [25] Wang, D., & Mota, D., 2021, Phys. Dark Universe, 100813.
- [26] Wu, C. H., Hu, Y. P., & Xu, H., 2021, Eur. Phys. J. C, 81(4), 1-9.
- [27] Horndeski, G. W., 1974, Int. J. Theor. Phys., 10(6), 363-384.
- [28] Guo, M., & Li, P. C., 2020, Eur. Phys. J. C, 80(6), 1-8.
- [29] Berti, E., Collodel, L. G., Kleihaus, B., & Kunz, J., 2021, Phys. Rev. Lett., 126(1), 011104.
- [30] Antoniou, G., Bakopoulos, A., & Kanti, P., 2018, Phys. Rev. D, 97(8), 084037.
- [31] Maeda, K. I., Ohta, N., & Sasagawa, Y. 2009, Phys. Rev. D, 80(10), 104032.
- [32] Bekenstein, J., & Milgrom, M., 1984, Astrophys. J., 286, 7-14.
- [33] Doneva, D. D., & Yazadjiev, S. S., 2021, J. Cosmol. Astropart. Phys., 2021(05), 024..
- [34] Fernandes, P. G. (2020), Phys. Lett. B, 135468.
- [35] Bean, R., Flanagan, E. E., & Trodden, M. 2008, Phys. Rev. D, 78(2), 023009.
- [36] Khoury, J., & Weltman, A., 2004, Phys. Rev. D, 69(4), 044026.
- [37] Folomeev, V., Aringazin, A., & Dzhunushaliev, V., 2013, Phys. Rev. D, 88(6), 063005.
- [38] AGHANIM, N. et al. Planck 2018 results-VI. Cosmological parameters. Astron. Astrophys., 2020, vol. 641, p. A6.
- [39] Yavetz, T. D., Li, X., & Hui, L., 2022, Phys. Rev. D, 105(2), 023512.
- [40] Matos, T., & Urena-Lopez, L. A., 2000, Class. Quantum Gravity, 17(13), L75.
- [41] Arbey, A., & Coupechoux, J. F., 2021, J. Cosmol. Astropart. Phys., 2021(01), 033.

- [42] Stegmann, J., Capelo, P. R., Bortolas, E., & Mayer, L., 2020, *Mon. Not. Roy. Astron. Soc.*, 492(4), 5247-5260.
- [43] Meszaros, P., 1974, *Astron. Astrophys.*, 37, 225-228.
- [44] Hawkins, M. R. S., 2020, *Astron. Astrophys.*, 633, A107.
- [45] Bernal, N., & Zapata, Ó., 2021, *J. Cosmol. Astropart. Phys.*, 2021(03), 015.
- [46] Belotsky, K. M., et al., 2019, *Eur. Phys. J. C*, 79(3), 1-20.
- [47] Ludlow, A. D., et al., 2014, *Mon. Not. Roy. Astron. Soc.*, 441(1), 378-388.
- [48] Brownstein, J. R., & Moffat, J. W., 2006, *Astrophys. J.*, 636(2), 721.
- [49] Lelli, F., 2022, *Nat. Astron.*, 1-13.
- [50] Strigari, L. E., et al., 2008, *Astrophys. J.*, 678(2), 614.
- [51] Carr, B., Kohri, K., Sendouda, Y., & Yokoyama, J. I., 2021, *Rep. Prog. Phys.*, 84(11), 116902.